Using the artificial neural network to investigate the effect of parameters in square cup deep drawing of aluminum-steel laminated sheets

M. Mahmoodi *[1], H. Tagimalek [2], H. Sohrabi [3], M. R. Maraki [4]

[1,2,3] Faculty of Mechanical Engineering, Semnan University, Semnan, Iran
[4] Department of Materials and Metallurgy Engineering, Birjand University of Technology, Birjand, Iran

Abstract

In this study, the effective parameters involved in the deep drawing of double-layer metal sheets in a die of square cross-section were investigated through artificial neural network (ANN) modeling. For this purpose, first, the deep drawing of double-layer (Al1200 / ST14) sheets was carried out experimentally. Also, the finite element simulation of the process was performed, and the results validated through experimental tests. A set of 46 different experimental data were employed in this paper. The ANN was trained by using a mean square error of 10^{-4}. The input parameters, i.e., punch radius, die radius, blank holder force, clearance, and the permutation layers were set to the network. The surface response method (RSM); was employed to evaluate the results of the ANN model, and the input parameters of the deep drawing process on the thinning of Al1200 and ST14 composite layers were analyzed. The obtained results indicate that the punch edge radius has the most significant influence on the thinning of the Al1200 layer. Increasing the gap between the punch and die to 1/4 of the sheet thickness, increased the cup wall layers thickness of the Al1200 and ST14 respectively by 3.38% and 0.5%. The performance of the ANN model demonstrates that it can estimate the amount of thinning in the composite layers with satisfactory accuracy.

Keywords: Square cup deep drawing, Aluminum, Steel, Composite, Artificial neural network.

1. Introduction

Deep drawing is a sheet metal forming process used in various industries [1)]. The deep drawing of double-layer metal sheets can be used to manufacture parts with different interior and exterior properties (e.g., resistance to corrosion and friction and electrical and thermal conductivities) [2-3)]. Because of various products, the deep drawing process has found numerous applications in industries related to auto manufacturing, aerospace, medical devices, and electronics [4)].

Artificial intelligence (AI) [5)] and design of experiments (DoE) [6)] are widely used in complex modeling. In recent years, the artificial neural networks (ANN) have been used in numerous areas, including the estimation and prediction of functions. An ANN is a type of information processing technology, and it can efficiently solve the problems in which a complex nonlinear relationship exists between the input and output variables. The use of ANN, as a new method of predicting the nonlinear behavior of materials, is a cheaper, more

**Corresponding author*
Email:mahmoodi@semnan.ac.ir
Address: Faculty of Mechanical Engineering, Semnan University, Semnan, Iran
1. Assistant Professor
2. PhD Candidate
3. M.Sc
4. M.Sc

accessible, more efficient, and more reliable substitute for estimating the mechanical properties of materials using data obtained from experimental tests [7-8].

Mahdavian et al. [9] investigated the effect of punch profile (shape) on the deep drawing of circular section aluminum sheets. In each of the performed experiments using a deep drawing die apparatus, they measured the Aluminum sheet holder force and the punch movement to examine the effects of different parameters on the deep drawing process. They concluded that the punch geometry affects the friction between the blank and the punch. Li et al. [10] studied the delamination phenomenon in the deep drawing of double-layer metal sheets. They considered the viscoelastic behavior for the mechanical properties of the glue model and the connected elements. According to their findings, wrinkling leads to the delamination of double-layer metal sheets. Wang et al. [11] employed the surface response method and finite element analysis to control the strain path during the forming process by applying different plate holder forces. Delmezier et al. [12] used the optimized material properties of thin sheets in the deep drawing process. They considered two material properties in their studies, namely the work hardening and the average anisotropy coefficient. They also used the surface response method to define two objective functions (i.e., rupture and wrinkling) for controlling the forming flaws. The surface response approach establishes a limited number of assessments for the objective functions, which are used in determining the optimal material properties. Singh et al. [13] employed a neural network and genetic algorithm (GA); to identify the optimal parameters in the deep drawing of circular sheet blanks. They conducted 28 tests to obtain the needed information for the training of the ANN. The output of their tests was the thickness of the samples obtained from each experiment; at two critical points. Manoochehri et al. [14] used a neural network and the annealing algorithm to optimize the deep drawing process. Their objective was to model and optimize the input parameters of the deep drawing process for SS304. Morrovati et al.[15] performed research on optimizing the initial shape of multilayer metal sheet blanks used in deep drawing. For this purpose, they employed the GA and ANN along with the FE simulation. In their research, the ANN predicts the final shape of the blank after its deformation, and the GA proposes the most optimum form of the initial blank. Hosseini et al. [16] published a paper titled using the ANN-FE approach to adjust the gap between the plate holder and the die surface during the impact of a punch in the deep drawing of circular sheet blanks. They demonstrated that choosing a proper gap between the plate holder and the die surface helps achieve a uniform thickness throughout the sample wall and a greater depth in the sample. Takala et al. [17] investigated the effects of process parameters to eliminate the defects like tearing, wrinkling, earing, and spring-back. The study also focuses on the deep drawing of the composite sandwich materials at the elevated temperatures. The different behaviors are observed for different materials at high temperatures. Mahmood et al. [18] studied the flexible square cup deep drawing process of micro SS304. The results showed that the initial foil thickness affects the thinning and thickening values of the formed cup wall. The optimization method is feasible to indicate the optimum initial blank shape for producing free flange-micro square parts. Reddy et al. [19] analyzed the deep drawing process of rectangular cups made of different anisotropic materials. The experiments were performed by designing deep drawing tools such as die, blank holder, and punch. Also, the numerical simulations performed for deep drawing of rectangular cups using two levels of parameters like lubricating condition and blank material.

In this paper, the deep drawing of a double-layer (Al/ST) sheet inside a die with a square cross-section has been modeled by the finite element method. The obtained simulation results have been validated through experimental tests. In order to model this process and to achieve the maximum amount of thinning in the wall of the obtained sample, 46 experiments with different inputs have been designed using the ANN; these tests have been performed by using the FE method and, ultimately, the ANN has been trained using these data. Then, by using the achievements of this research, i.e., the ANN model of the process with the maximum amount of thinning in the sample, and by employing the surface response method, the effects of the input parameters of the deep drawing process on the thinning flaw have been determined.

2. The experimental process

A deep drawing dies with a square cross-section was used to perform the experimental tests (Fig 1). The specially designed die was used because of the forces involved in the workpiece and the slipping of the sheet.

As is observed, this die system consists of a punch, a die, a blank holder mechanism with adjustable holding force, bushing, and guide rods. The mechanical properties of the examined steel-aluminum sheets were shown in Fig. 2 and table. 1.

The dimensions of the original aluminum-steel blanks were 85×85×0.7 mm^3. A hydraulic press with a 50-ton capacity provided the force needed to form the square shape cups. The punch moves to a depth of 15 mm to plastically deform the blanks.

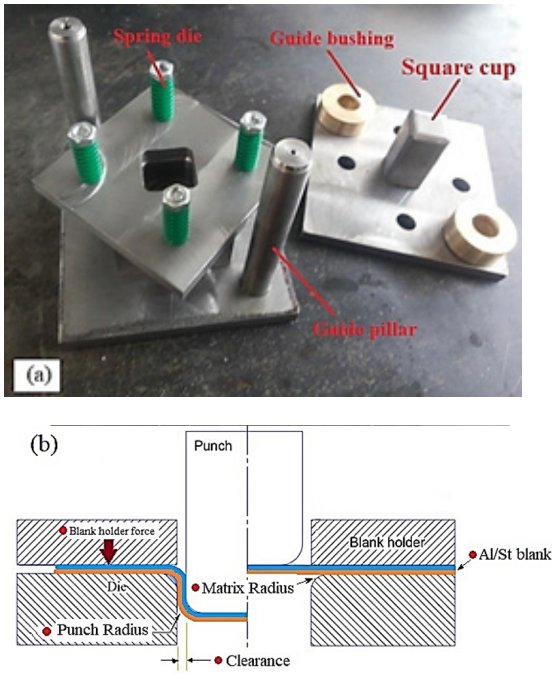

Fig. 1. a) Experimental square section die set up b) Schematic the process and input parameters.

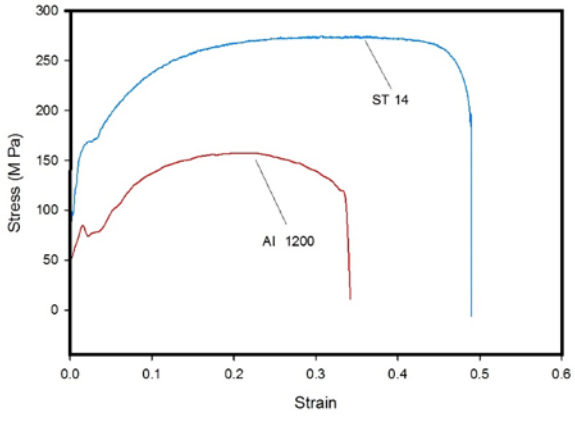

Fig. 2. Engineering stress-strain curves for ST14 and Al1200.

Table 1. Mechanical Properties of ST14 and Al1200.

	Young's modulus (GPa)	Poisson's Ratio	Density (Kg/m^3)
ST 14 steel	210	0.3	7800
Al-1200	75	0.33	2710

3. Finite element simulation of the deep drawing process

The ABAQUS software package has been used to perform the numerical simulation of the deep drawing of double-layer metal sheets. The model shown in Fig. 3 is a three-dimensional designed model. Due to the symmetry of the sample's geometry, only one-quarter of

the overall geometry needs to be analyzed. The double-layer sheet consisting of Al1200 and steel ST14 was designed in a shell form. The components of the die assembly, including the punch, blank holder, and die, were modeled as rigid elements. Moreover, the Dynamic-Explicit analytical method employed in this research.

The two-layer sheet was modeled in Shell planar by Four-node shell elements (S4R), and the "Tie" constraint was defined to tie two separate surfaces together so that there is no relative motion between them. This type of constraint allows fusing two regions [20].

The meshes applied to all the die and double-layer sheet components have a quad form, and a structured technique was used in this model. Table 2 shows the types of elements and the specifications of the die components and double-layer sheets used in the simulations.

4. Designing and training the artificial neural network

One of the objectives of this paper is to evaluate the quality of the final sample obtained in the mentioned deep drawing process by the ANN. The neural network has been trained using the data obtained from the numerical simulation of the process by the ABAQUS software. 46 test data were utilized to train the neural network. Each test sample had five inputs and two outputs. The effective process parameters were considered as the input parameters of the network (given in Table 3).

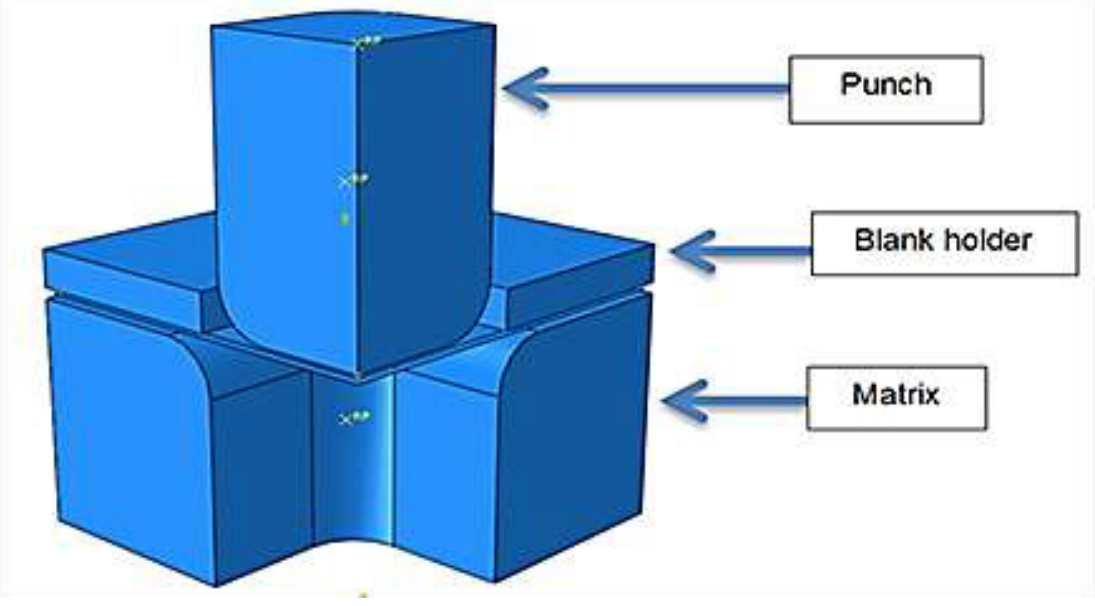

Fig. 3. Geometrical model of the die.

Table 2. Specifications of the meshes and elements used in the simulations.

Part name	Nodes number	Element type	Properties type
Punch	Four node	R3D4	Rigid
Blank holder	Four node	R3D4	Rigid
Double layer sheets	Four nodes decreased	Shell - S4R	Deformation
3	Four node	R3D4	Rigid

Table 3. Input parameters of the neural network.

Levels	Matrix radius	Punch radius	Blank holder force	Clearance (t= sheet thickness)	Permutation layer
Unit	(mm)	(mm)	(Newton)	(mm)	(top-down)
1	3.35	5.35	2000	1.1t	Al-ST
2	4.35	6.35	4000	1.2t	ST-Al
3	5.35	7.35	6000	1.3t	--
4	6.35	8.35	8000	1.4t	--

Two outputs were extracted from each Experiment. The first output relates to the maximum amount of thinning in the aluminum layer, and the second output is the maximum thickness reduction in the steel layer. Since the initial thickness of the sheets is 0.7 mm, the values associated with the selected quality index are all less than the initial sheet thickness, and the ideal case would be the one in which these values are closer to 0.7. Thus, 46 experiments were performed, with the specifications given in Table 4.

Table 4. Results of simulation analysis as the input data for the ANN.

Input						Output	
Test number	Matrix edge radius	Punch edge radius	Blank holder force	Clearance	Permutation layers	Maximum thinning in the aluminum layer	Maximum thinning in steel layer
1	1	1	1	1	1	0.5466	0.6073
2	1	2	2	2	1	0.5694	0.6151
3	1	3	3	3	2	0.5532	0.6236
4	1	4	4	4	2	0.5578	0.6244
5	2	1	2	3	2	0.5020	0.6032
6	2	2	1	4	2	0.5352	0.6175
7	2	3	4	1	1	0.5857	0.6233
8	2	4	3	2	1	0.6038	0.6288
9	3	1	3	4	1	0.5623	0.6083
10	3	2	4	3	1	0.5805	0.6179
11	3	3	1	2	2	0.5861	0.6308
12	3	4	2	1	2	0.6009	0.6334
13	4	1	4	2	2	0.4905	0.6060
14	4	2	3	1	2	0.5549	0.6237
15	4	3	2	4	1	0.6083	0.6277
16	4	4	1	3	1	0.6323	0.6340
17	3	4	1	4	2	0.6075	0.6351
18	3	3	2	2	1	0.6065	0.6264
19	2	3	4	2	2	0.5808	0.6281
20	2	2	2	3	1	0.5776	0.6173
21	1	2	4	1	1	0.5562	0.6133
22	1	3	4	3	2	0.5470	0.6213
23	1	4	2	4	1	0.5971	0.6267
24	2	1	3	4	2	0.4837	0.5993
25	3	1	3	3	1	0.5592	0.6092
26	4	3	1	2	2	0.5937	0.6322
27	4	2	2	2	2	0.5548	0.6242
28	4	4	4	4	1	0.6193	0.6321
29	2	3	2	1	2	0.5731	0.6287
30	1	1	1	3	2	0.5010	0.6003
31	4	1	4	1	1	0.5718	0.6126
32	3	2	3	2	2	0.5328	0.6187
33	3	1	4	4	1	0.5642	0.6073
34	3	4	2	3	2	0.6026	0.6335
35	2	3	1	3	1	0.5884	0.6254
36	1	4	3	2	1	0.5929	0.6258
37	1	2	3	2	1	0.5664	0.6134
38	1	3	1	2	2	0.5551	0.6276
39	2	4	3	4	2	0.5804	0.6297
40	2	1	4	2	1	0.5563	0.6067
41	3	3	1	1	2	0.5881	0.6319
42	3	2	4	1	1	0.5764	0.6199
43	4	2	1	2	1	0.6026	0.6236
44	4	3	2	3	2	0.5919	0.6316
45	4	4	1	2	2	0.6190	0.6370
46	4	3	3	3	1	0.6080	0.6278

The trained ANN has two layers in the hidden layer section, with 10 and 15 neurons allocated to the first and second layers, respectively. The lower and upper limits of the permitted number of neurons assigned to the layers were obtained from Eq.1.

$$2(n_i + n_0) \leq n_1 \leq \frac{k(n_i + n_0) - n_0}{n_i + n_0 + 1} \qquad \text{Eq.(1)}$$

In the above equation, n_1 is the number of neurons in the first layer, n_i is the number of inputs, n_0 is the number of outputs, and k is the number of test samples, which in this research is 46, according to Table. 4. The process of modeling the ANN is summarized in Fig 4.

Table. 2 shows the trial and error procedure for finding the optimal structure of the ANN for estimating the amount of thinning in the double-layer sheet resulting from the deep drawing of square blanks. In this procedure, the mean squared error and the fitting coefficient were computed and compared for ANN with different structures (different numbers of hidden layers and neurons) and, finally, a network with the most negligible value of mean squared error and the largest fitting coefficient was selected as the ANN with the best performance.

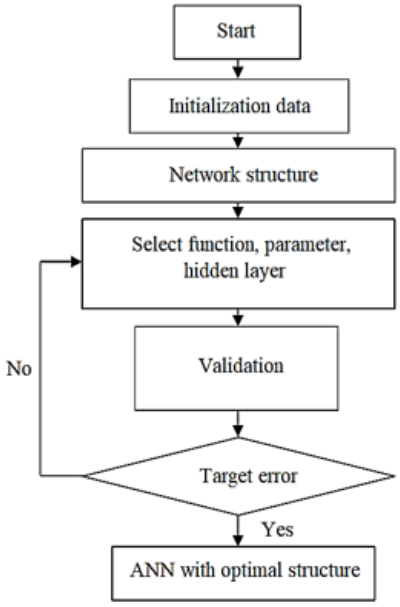

Fig. 4. The process of modeling the ANN.

Table 5. Process of trial and error for finding the optimal numbers of hidden layers and neurons.

Hidden layers	Neurons in each hidden layer	Mean error squares	Fitting coefficient
1	2	4.6127	0.98639
1	3	4.3678	0.98715
1	4	0.7603	0.99723
1	5	0.4275	0.99849
1	6	0.1537	0.99934
1	7	0.5873	0.99784
1	8	0.5398	0.99746
1	9	0.4653	0.99828
1	10	0.5113	0.99788
2	2	2.0379	0.99362
2	3	2.6176	0.99118
2	4	0.4797	0.99839
2	**5**	**0.0172**	**0.99986**
2	6	0.1225	0.99951
2	7	0.3373	0.99869
2	8	0.8355	0.9975
2	9	0.4122	0.99819
2	10	1.6592	0.99045

By analyzing the performances of various networks, the multilayer perceptron network with two hidden layers and five neurons in each of those layers was selected as the network with the best performance. As is observed in Table 5, the mean squared error of the selected network (0.0172) is the lowest value, compared to the other networks. Also, the fitting coefficient is very close to 1.0, which indicates the good performance of the selected ANN. The modeled ANN was illustrated in Fig. 5.

A tan-sigmoid transformation function was used in both hidden layers (Fig. 6). The role of a transfer function is to compute the output of a layer from its input. The mathematical form of this function was given in Eq. 2.

$$Tansing(n) = (2/(1 + ext(-2^n))) - 1 \qquad \text{Eq.(2)}$$

70% of the data was allocated for the training of the ANN. 15% of the data was considered for validation, and the remaining 15% considered for testing the ANN.

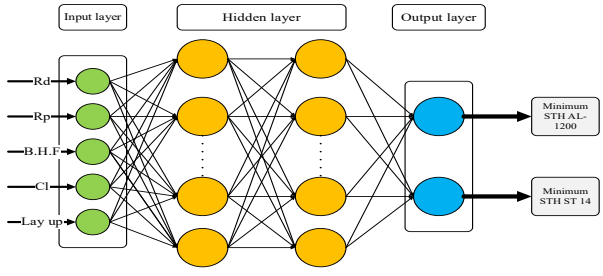

Fig. 5. Multilayer network with two hidden layers, with 15 neurons in the first layer and ten neurons in the second layer.

The ANN was trained by the Levenberg-Marquardt (trail) algorithm. Fig. 7 shows the performance of the modeled ANN versus the scattering of test, training, validation, and total data. The network's performance was measured by the mean squared error, which has an upper limit of 10^{-4}, and as this limit is reached, the network's behavior stops changing. These graphs clearly show the matching of empirical (target) data with the outputs of the ANN. The regression diagram and the fitting coefficients for the data indicate a lack of over-fitting and under-fitting errors and point out the proper training of the ANN. Since the scattering of the total data is above 0.9, it can be concluded that the data obtained from the simulation of the ANN are valid and reliable.

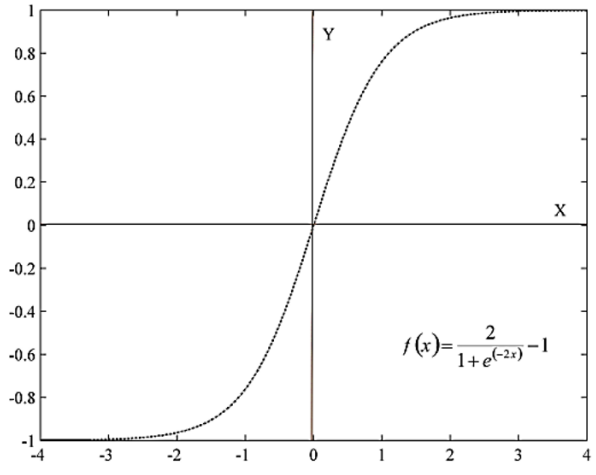

Fig. 6. Tan sigmoid transformation function.

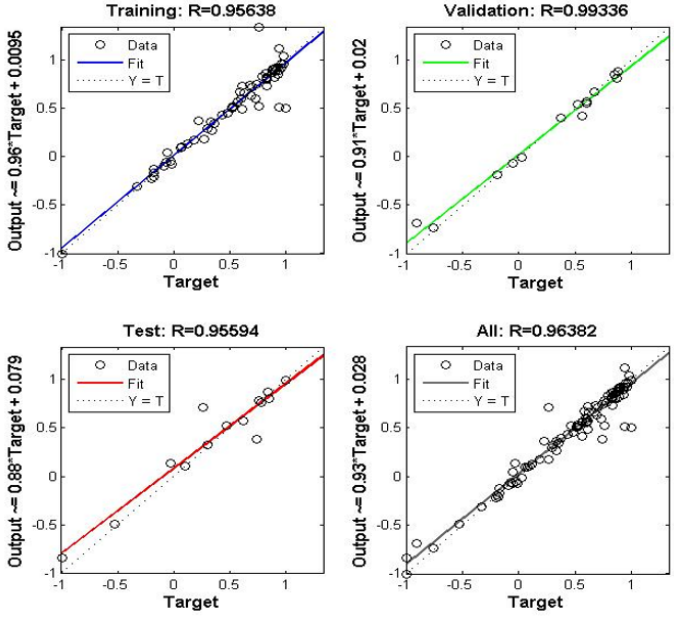

Fig. 7. Distribution of the neural network data based on the mean squared error criterion.

5. Results and discussion

5.1. Validation of results

Fig. 8 shows the thickness variations along the two directions defined based on the experimental and simulations. It is observed that maximum thinning occurs in the radial region of the punch and along path B. Thus, this direction has been used for validation purposes and for analyzing the thickness changes.

This graph also shows that the highest amount of thinning in the aluminum layer is 3% more than that in the steel layer, which is the bottom layer of the fabricated cup.

Fig. 9 shows the distributions of thickness in the wrinkled cup, in the Al and ST layers, and along with path B, based on the experiments and simulations. In the experimental work, maximum thinning occurs in the radial region of the punch and in agreement with the simulation. In the practical work, the maximum amounts of thinning in the Al and ST layers are 21% and 16.6% of the initial sheet thickness respectively. For the Al and ST layers, these values are 7.09% and 5.7% higher than the maximum thinning values obtained in the simulation work.

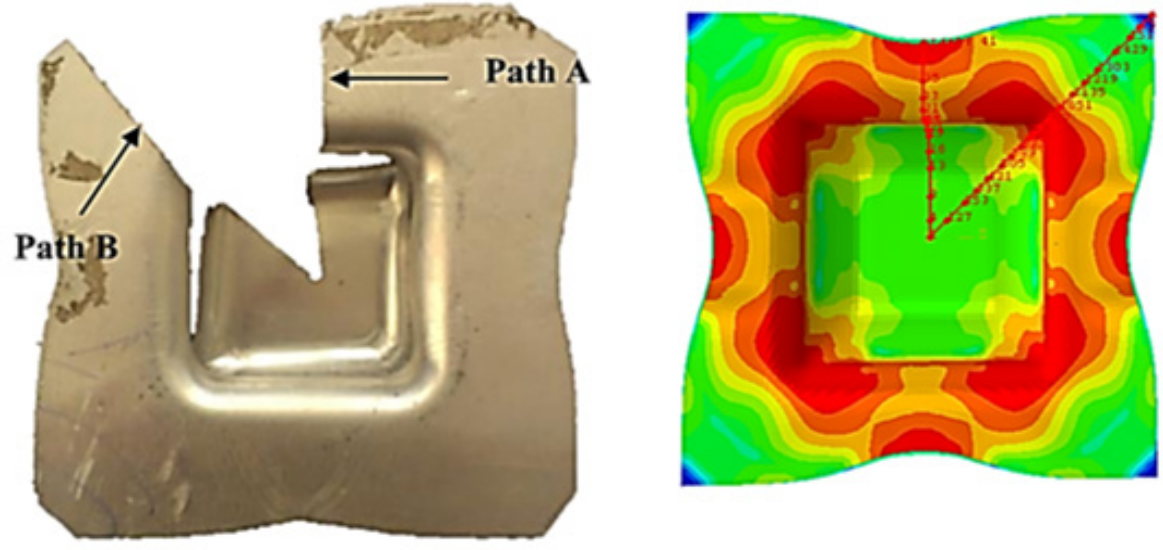

Fig. 8. Paths A and B determined for measuring the thickness variations.

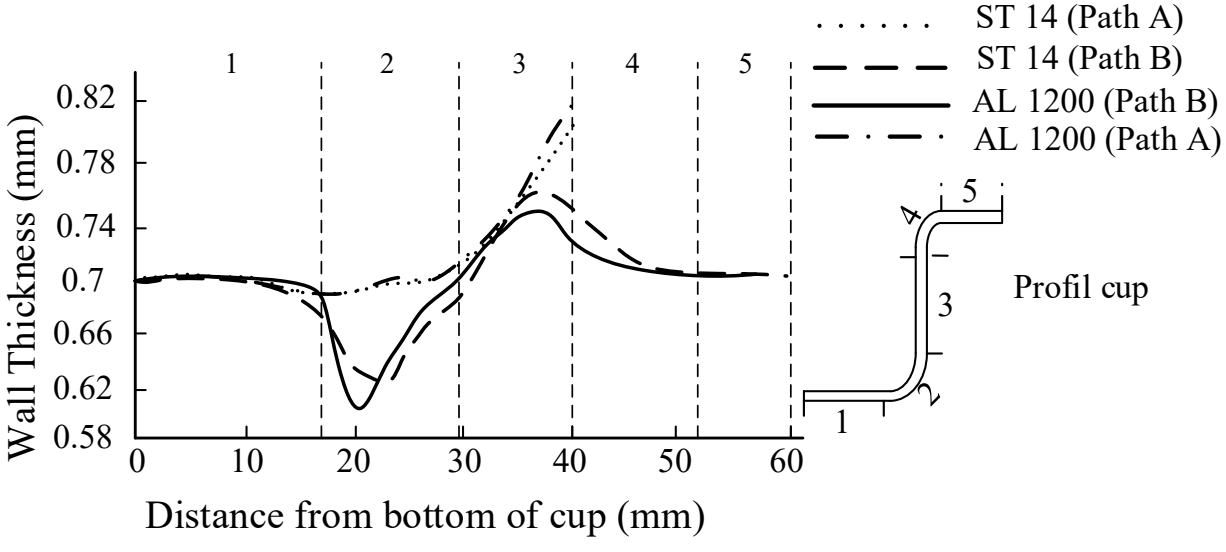

Fig. 9. Graph of thickness distribution obtained through simulation, along the two paths and in the two materials used in the wrinkled cup.

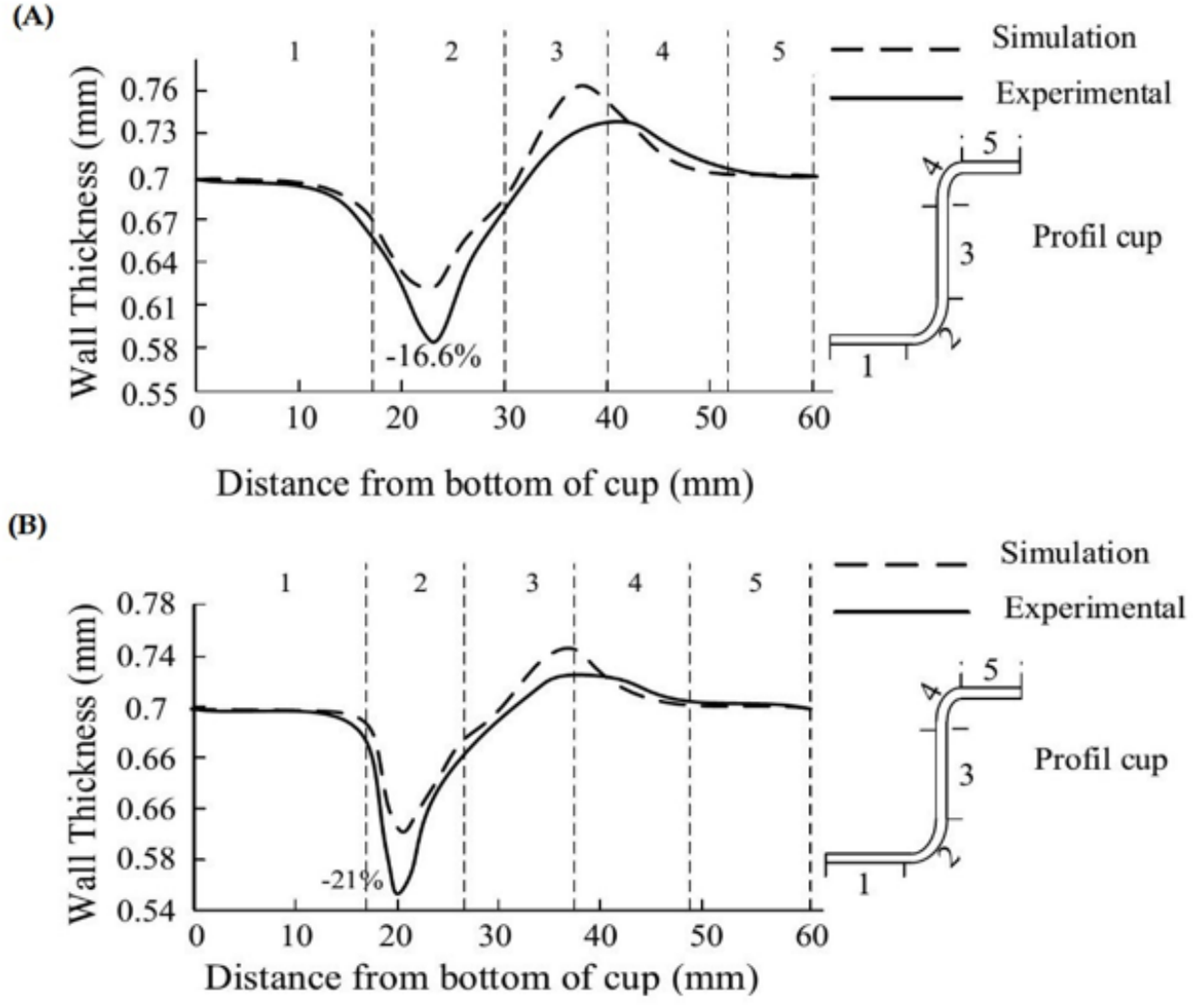

Fig. 10. Thickness variations in the (A) steel and (B) aluminum layers of the wrinkled cup, based on the experimental work and the simulation along path B.

The design of experiments by the surface response method has been employed in this research to analyze the effects of the governing input parameters on the deep drawing process. The examined output is the maximum amount of thinning in the Al and ST layers which is also considered as an index for the onset of damage.

Reddy et al. [19] showed for all the cups that the stress formation zone is along with the corners of the cup. With the help of forming limit diagram (FLD), the strain condition for the fracture risk element can be used to evaluate the Feasibility of the forming process [9]. In this work, a square blank was used. According to Morovvati et al. work [15], using an optimal blank shape, a reduction of about 12% in the deformation force is seen in the deep drawing process for a cup. Furthermore, the thickness difference decreases for stainless steel and Al 1100, and the uniformity of strain distribution highly increases in the forming process.

Fig. 10 shows the effect of die edge radius on the thickness of the aluminum layer. It is observed that, with a 47.2% increase in the die shoulder radius, the thicknesses of the Al and ST layers also increase by 5% and 3.96%, respectively. Therefore, with the increase of die shoulder radius, sheet flow will improve in this radial region, and consequently, less thinning will occur in this section. Thus, a die radius of 6.35 mm can be considered a suitable radius for improving the deep drawing process. The thinning of the steel layer diminishes by 1.04% relative to the aluminum layer.

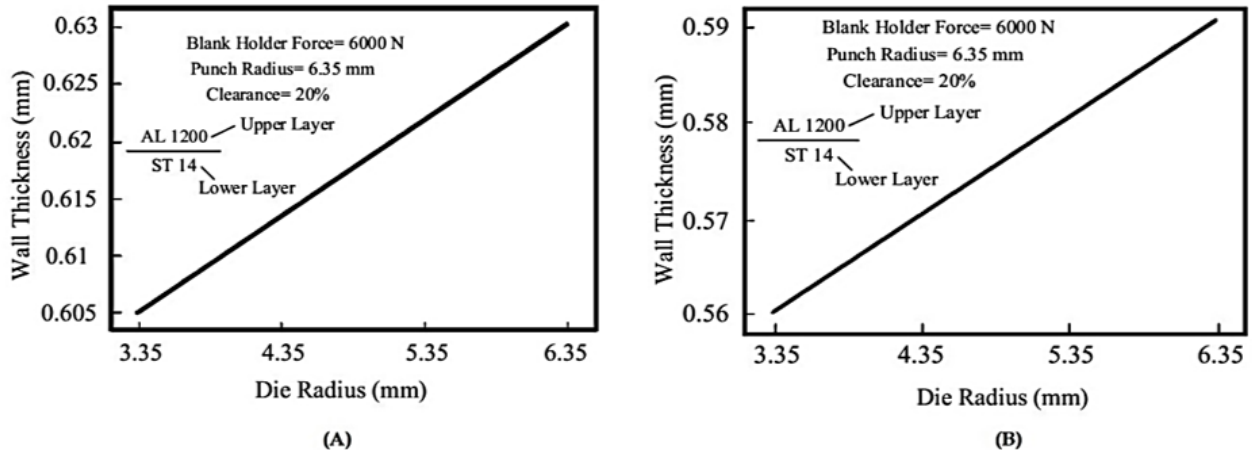

Fig. 11. Effect of die shoulder radius on the thickness of (A) steel and (B) aluminum layer in the cup wall.

Fig. 11 shows the effect of punch edge radius on the thickness of the Al1200 and the ST14 layers. It is observed that with a 35.9% increase in the punch radius, the thicknesses of the Al and ST layers also linearly increase by 5.75% and 0.95%, respectively. This is due to the easier flow of the sheet material inside the die cavity, which reduces the thickness variations and the share of sheet stretching in this radial region. Based on these results, a punch radius of 8.35 mm can be considered a suitable radius for improving the flow of the blank material and reducing the amount of thinning. The amount of thinning in the steel layer has diminished by 4.8% compared to the aluminum layer. This matter indicates that, despite the higher strength of the steel layer relative to the aluminum layer, because of the arrangement of these layers, the steel layer, which constitutes the outer layer of the cup, undergoes more stretching than the upper (Al) layer. However, steel is stronger than aluminum and the thickness increase of the steel layer is also less than that of the aluminum layer. Another parameter to consider is the thinning of a layer relative to the initial thickness of the raw blank. In the conducted investigations, due to the lower tensile strength of aluminum, the amount of thinning in aluminum layers relative to the initial sheet thickness has always been less than that in steel layers. Adnan et al. [21] showed that the work is more affected by the die profile radius than the punch profile radius. This is attributed to the work consumed in the plastic deformation being much more in the case of the die profile radius. The great majority of the sheet will be formed over the die profile radius (the part which forms the cup wall) as compared to a small part of the sheet which will form over the punch profile radius.

Fig. 12 illustrates the effect of blank holder force on the thickness of Al and ST layers. It is observed that with a 75% increase in the blank holder force, the thicknesses of the Al and ST layers in the cup wall are reduced by 2.5% and 2.3%, respectively. This amount diminishes in the steel layer by 0.2% relative to the aluminum layer; because the increase of the blank holder force does not

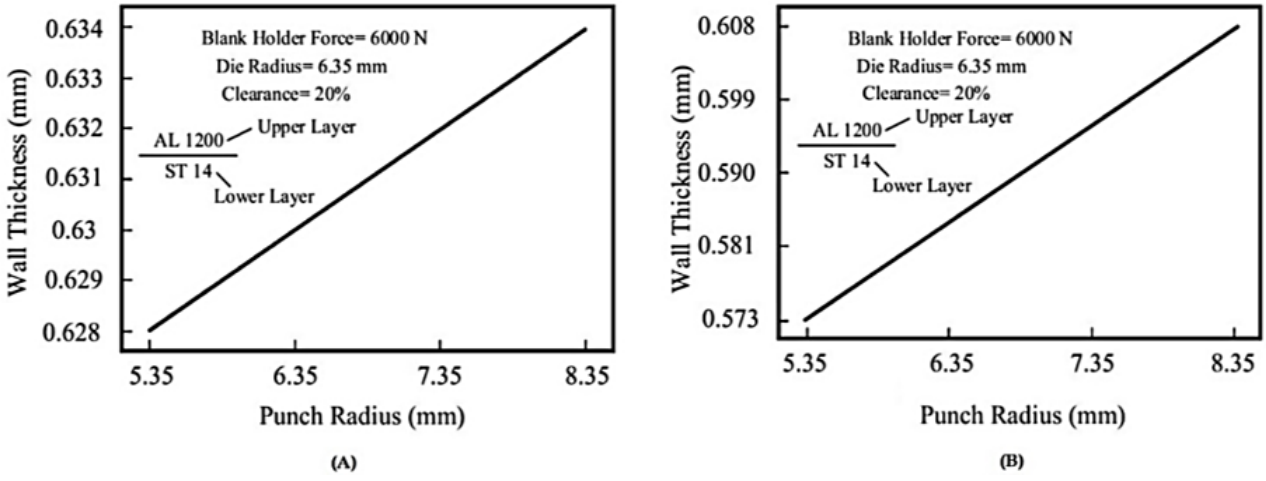

Fig. 12. Effects of punch nose radius on the thickness of (A) steel and (B) aluminum layer in the cup wall.

allow the sheet to flow from the edge region of the cup and, therefore, the length of the sheet material increases as a result of thinning in the cup wall. Consequently, the amount of thinning in the cup will increase with the increase of the blank holder force. Nevertheless, the blank holder force plays an important role in controlling the flow of the sheet material and eliminating the wrinkling in the edge region of the cup. So, by choosing an appropriate blank holder force, parts free of wrinkling and rupture can be fabricated. Since most of the BHF; is concentrated on the corners where the metal thickens more, the sides of the rectangle cannot get enough pressure to restrain the metal and prevent wrinkling. Increasing the blank holder pressure at the sides of the rectangular blank using a multipoint pressure control system may improve the formability of rectangular blanks. Control of the BHF; improves the formability and the quality of the final part.

Fig. 13 shows the effect of the gap between a punch and die on the thickness of the Al and ST layers in the cup wall. The gap considered in this work is based on the sheet's initial thickness, and the maximum amount of gap is taken as ¼ of the total sheet thickness. The findings of this Investigation indicate that by increasing the gap to ¼ of the sheet thickness, the thicknesses of the Al and ST layers also increase by 3.38% and 0.5%, respectively. So, this value has diminished by 2.88% in the steel layer relative to the aluminum layer. The increase of thickness, i.e., reduction of thinning, is less in the bottom layer than the top layer. The gap between a punch and die is an important parameter in the success of the deep drawing process. A small gap causes the ironing and severe thinning of the sheet in the die cavity and eventually leads to its rupture, while a large gap results in the wrinkling of the cup walls. Therefore, for a successful deep drawing operation, it is necessary to determine a suitable gap value. It is usually 25% of the initial sheet thickness.

Fig. 14 shows the effects of the process parameters on the obtained empirical results. Choosing incorrect parameter values will lead to the rupture or wrinkling of the double-layer sample. This wrinkling can be avoided by selecting the correct blank holding force (BHF), reduced friction, increasing the tool edge radius, and reducing the deep drawing depth all together in one operation. Fracture defect is eliminated with proper chosen BHF.

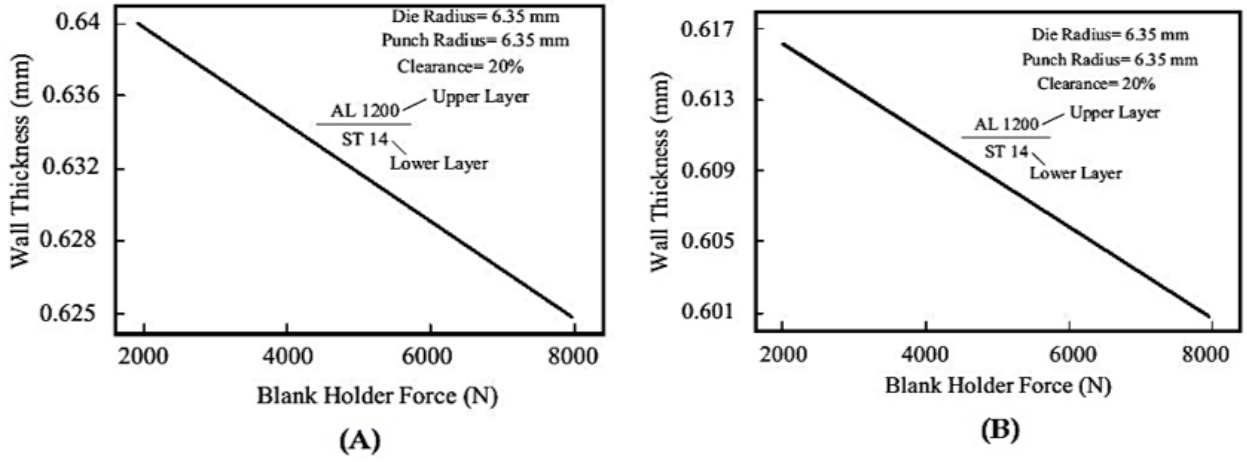

Fig. 13. Effect of blank holder force on the thickness of (A) steel and (B) aluminum layers in the cup wall.

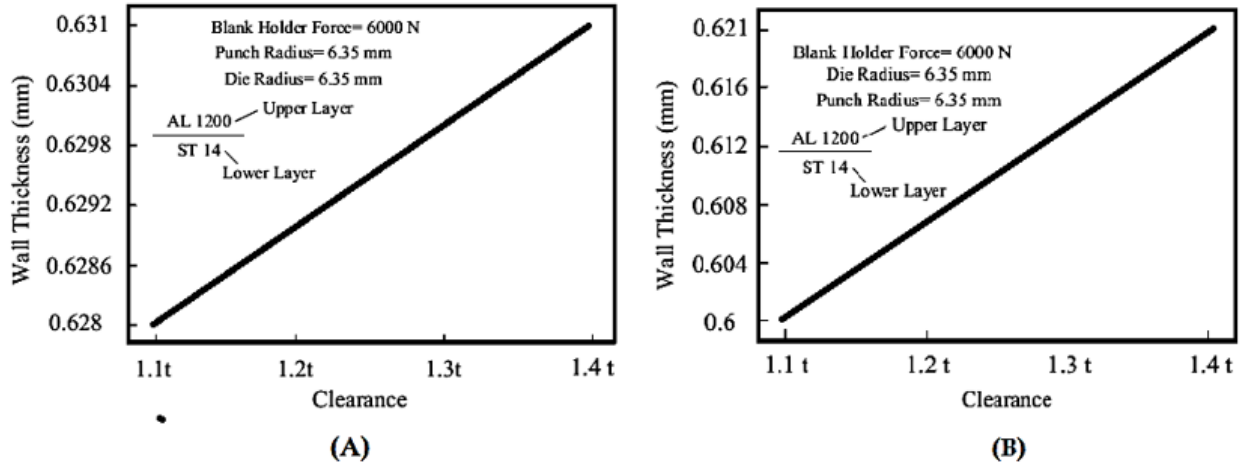

Fig. 14. Effects of the gap between a punch and die on the thickness of the (A) steel and (B) aluminum layers in the cup wall.

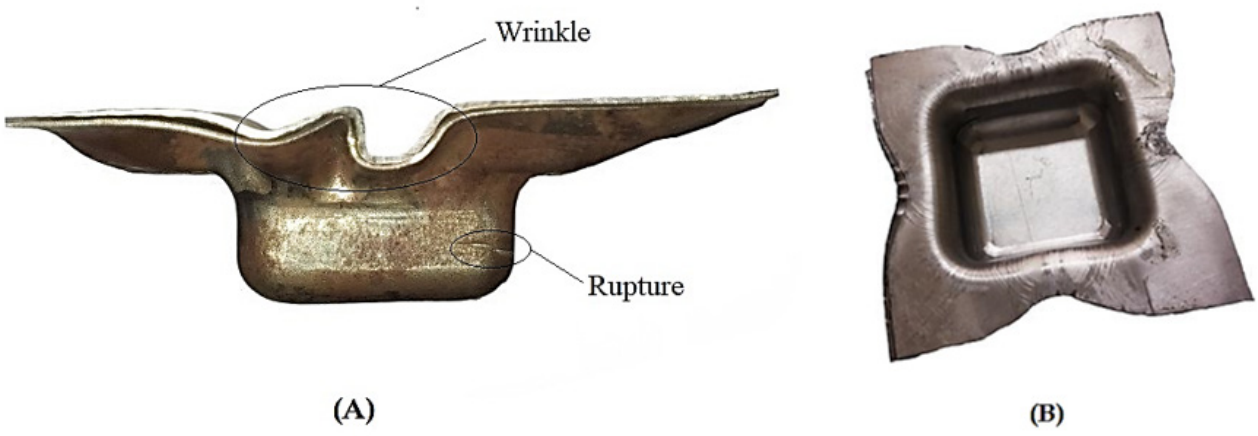

Fig. 15. Comparing an (A) wrinkled or ruptured sample with a (B) flawless sample obtained from the deep experimental drawing of a square double-layer sheet.

6. Conclusion

In this paper, 3D finite element simulations and experimental tests have been used to explore the deep-drawing of double-layer sheets of aluminum 1200 and steel ST14 in a die with a square cross-section. Finite element simulation, has been validated through experimental deep drawing operations and to collect different thinning output data needed for the training of the ANN. A multilayer ANN and the surface response method have been used to analyze the amount of thinning in the double-layer sample with a square cross-section. The performance of the ANN indicates that it can estimate the amount of thinning in the sample with satisfactory accuracy. The obtained results indicate that by employing the mathematical models, especially the ANN model, the effects of the process parameters involved in the deep drawing of square section samples can be investigated without costly and time-consuming tests and experiments. An examination of thickness distribution in the sample layers shows that the maximum amount of thinning occurs in the radial region of the punch and along with path B (Fig. 9.) Also, the effects of the input parameters of the deep drawing process on the percent thinning of the Al and ST layer are as follows:

- With a 47.2% increase in the die shoulder radius, the thicknesses of the Al and ST layers increase by 5% and 3.96%, respectively.
- With a 35.9% increase in the punch edge radius, the thicknesses of the Al and ST layers increase by 5.75% and 0.95%, respectively.
- With a 75% increase in the blank holder force, the thicknesses of the Al and ST layers in the cup wall diminish by 2.5% and 2.3%, respectively.
- By increasing the gap between a punch and die to ¼ of the sheet thickness, the thicknesses of the Al and ST layers in the cup wall increase by 3.38% and 0.5%, respectively.

References

[1] L.H. Zhang, Z.J. Wang, Z. Wang: Inter Jour of Mech Sci., 159 (2019), 498.
[2] J. Lu, Y. Song, L. Hua, P. Zhou, X. Gwangju: Tribol Inter., 140 (2019), 105872.
[3] R. Zhao, J. Steiner, K. Andreas, M. Merklein, S. Tremmel: Tribol Inter., 118 (2018), 488.
[4] J. Herrmann, M. Merklein: Pro Manu., 15 (2018), 980.
[5] M.R. Maraki, H. Tagimalek, M. Azargoman, H. Khatami, M. Mahmoodi: Inter Jour of Eng., 33 (2020), 2526.
[6] H. Tagimalek, M.R. Maraki, M. Mahmoodi, M. Azargoman: Jour of App and Com Mech, 10.22055/JACM. 2019.31017.1811.
[7] J. Tenner, K. Andreas, A. Radius, M. Merklein: Pro Eng, 207 (2017), 2248.
[8] F. Lambiase, A. Paoletti: Jour of Manu Pro, 31 (2018), 820.
[9] S.M. Mahdavian, Y.T.M. Fion: Mater and Manu Pro, 22 (2007), 901.
[10] H. Li, J. Chen, J. Yang: The Inter Jour of Adv Manu Tech, 68 (2013), 647.
[11] L. Wang, T.C. Lee: Jour of Mater Pro Tech, 167 (2005), 452.
[12] A. Delameziere, H. Naceur, P. Breitkopf, C. Knopflenoir, J.L. Baton, P. Villon: Inter comm in Heat and Mass Tran, 3 (2002), 97.
[13] D. Singh, R. Yousefi, M. Boroushaki: Inter Jour of Mech and Mech Eng, 5 (2011), 991.
[14] M. Manoochehri, F. Kolata: The Inter Jour of Adv Manu Tech, 73 (2014), 245.
[15] M.R. Morovvati, B. Mollaei-Mariani, M. Haddadzadeh: Jour of Manu Sci and Eng, 132 (2010).
[16] A. Hosseini, M. Kadkhodayan: The Inter Jour of

Adv Manu Tech, 71 (2014), 352.
[17] A.S. Takalkar, L.B.M. Chinnapandi: CIRP Jour of Manu Sci and Tech, 27 (2019), 63.
[18] Z.H. Mahmood, I.K. Irthiea, A.K. Ahmed: Mater tod: PROC, 24 (2019).
[19] P.V. Reddy, J. Ramesha, P.S. Rao, P.J. Ramulu: Mater tod: PROC, 5 (2018), 27175.
[20] H. Tagimalek, M.R. Maraki, M. Mahmoodi, P. Mohammadzadeh: Iran (Iran) Jour of Ene and Envir, 12 (2021) 152.
[21] I.O.Z. Adnan, F.A. Hashim: Inter Jour of Sci & Eng Res, 8 (2017), 387.